Downregulation of hexokinase 2 improves radiosensitivity of breast cancer

Dan Zhang, Hui Wang, Wenjing Yu, Feng Qiao, Xiaoyu Su, Huiqin Xu

Department of Nuclear Medicine, The First Affiliated Hospital of Anhui Medical University, Hefei 230022, China

Contributions: (I) Conception and design: H Xu; (II) Administrative support: None; (III) Provision of study materials or patients: None; (IV) Collection and assembly of data: D Zhang, H Wang, W Yu; (V) Data analysis and interpretation: F Qiao, X Su; (VI) Manuscript writing: All authors; (VII) Final approval of manuscript: All authors.

Correspondence to: Huiqin Xu. Department of Nuclear Medicine, The First Affiliated Hospital of Anhui Medical University, 218 Jixi Road, Lushan District, Hefei 230022, China. Email: hufan1975@126.com.

Background: Hexokinase 2 (HK2) is a major glycolytic enzyme that plays a critical role in the development of tumor metabolism. Triple negative breast cancers (TNBC) have high glycolytic activity and poor prognosis. This study explored the effect of HK2 on radiotherapy (RT) sensitivity of TNBC.

Methods: The knockdown of *HK2* genes in TNBC by lentiviral shRNA was confirmed by quantitative real-time polymerase chain reaction (qRT-PCR) and western blotting. In addition, the boosts of radiation therapy effects of TNBC accompanied by a reduction of *HK2* gene were determined by CCK-8, flow cytometry and colonic formation assays. (^{18}F)-fluorodeoxyglucose (^{18}F-FDG) uptake was used to evaluate tumor growth before and after radiation therapy *in vivo*.

Results: After administration of lentiviral shHK2, the expressions of HK2 proteins and mRNA were inhibited effectively. Following exposure to different doses of X-rays, the survival rate of cells and colony formation displayed a decreased trend and the cell apoptosis rate increased in the Lv-shHK2 group (P<0.05). In addition, (^{18}F)-fluorodeoxyglucose (^{18}F-FDG) positron emission tomography/computed tomography (PET/CT) imaging showed that compared with control, the maximum standardized uptake value (SUVmax) was lower in the Lv-shHK2 group.

Conclusions: Downregulation of HK2 improved the radiosensitivity of breast cancer (BC).

Keywords: Breast cancer (BC); Lv-shHK2; radiation; (^{18}F)-fluorodeoxyglucose positron emission tomography/computed tomography (^{18}F-FDG PET/CT)

Introduction

Breast cancer (BC) is the most commonly diagnosed cancer among US women. It is also the leading cause of cancer-related deaths in women worldwide (1). Moreover, BC is regarded as a heterogeneous disease presenting a variety of intrinsic differences with regard to biological characteristics and distinct clinical therapeutic interventions (2). It is generally known that BC possesses is categorized into four major subtypes according to molecular analysis. These include hormone receptor positive [estrogen receptor (ER) and progesterone receptor (PR)], human epidermal growth receptor 2 (HER2) positive and triple negative (ER, PR and HER2 negative, TNBC) BC (3,4). Approximately 15–20% of these BC subtypes are TNBC, which is defined by the lack of gene expression of ER and PR as well as HER-2. This subtype is associated with high recurrence rates and poor prognosis (5). To date, no genomic target of proven therapeutic utility against TNBC has been verified. The most significant metabolic hallmark of malignant tumors is accelerated glucose metabolism. Even with sufficient oxygen supply, cancer cells mainly depend on glycolysis rather than mitochondria oxidative phosphorylation

for energy production. This phenomenon is known as "Warburg effect" (6). Hexokinase 2 (HK2), which catalyzes the first committed step of glucose metabolism, is highly expressed in most tumor cells compared to normal cells (7). The high expression of HK2, which promotes glycolytic activity in cancer cells, can be testified by the use of (^{18}F)-fluorodeoxyglucose (^{18}F-FDG) positron emission tomography/computed tomography (PET/CT) scanning. ^{18}F-FDG, as a glucose analogue, is taken up by cancer cells and phosphorylated to form FDG-phosphate under the action of HK. This byproduct cannot be metabolized further and is hence detectable on PET imaging.

Radiotherapy (RT) is one of the local treatments for BC. However, the presence of hypoxic cells in tumors is the one of the primary factors that cause resistance to RT. The current study aims to explore the effect of HK2 on RT sensitivity of BC *in vivo* and *in vitro*.

Methods

Cell line and cell culture

Human BC MDA-MB231 was obtained from Type Collection of the Chinese Academy of Sciences (Shanghai, China). The cell line was cultured in DMEM (Hyclone) supplemented with 10% FBS (Gibco) at 37 ℃ in humidified atmosphere of 5% CO_2.

Reagents

shRNA targeting HK2 (shHK2) and a negative control shRNA (shNC) were synthesized by Hanbio Biotechnology (Shanghai, China). The sequence of HK2 shRNA (GATC CGCCACAACTGTGAGATTGGTCTCATTTTCAAG AGAAATGAGACCAATCTCACAGTTGTGGTTTTT TC) was inserted into BamHI and EcoRI sites of pHBLV-U6-Scramble-ZsGreen-Puro. Recombinant lentivirus was constructed by Hanbio Biotechnology (Shanghai, China). Mouse anti-human HK2 antibody was purchased from Abcam (UK). Cell counting kit-8 (cck-8) was purchased from Sangon Biotech (Shanghai, China). Annexin V-FITC/PI Apoptosis kit was purchased from Bestbio (Shanghai, China).

Recombinant lentivirus transfection

BC cells were seeded in six well plates at a density of 5× cells each dish and cultured for 12 h. The cells were then infected with either Lv-shHK2 or Lv-shNC at a multiplicity of infection (MOI) with 20 using polybrene (Hanbio, Shanghai, China) according to the manufacture's protocol. Forty-eight h after infection, the medium was replaced with selective medium containing 1.5 µg/mL puromycin (Sangon, Shanghai, China). The knockdown efficiency was calculated according to green fluorescence (GFP) positive cell to total cell ratio under fluorescence microscope. Subsequently, stable infected cell lines were detected for HK2 expression and used for irradiation (IR) in relevant experiments.

Quantitative real-time polymerase chain reaction (qRT-PCR)

Twenty-four h after injection with lentivirus, total RNAs were extracted with Trizol reagent (Invitrogen, USA), and then reverse transcribed into cDNA by using PrimeScriptTMRT Master Mix kit (Code No. RR036A, TaKaRa, Japan) according to manufacturer's protocol. After the reverse transcription reaction at 37 ℃ for 15 min and 85 ℃ for 5 s, cDNA was synthesized. The PCR reaction was ten performed using SYBR Premix Ex TaqTM II kit (Code No. RR820A TaKaRa, Japan) on an ABI 7500 thermal cycler (Applied Biosystems). Initial denaturation at 95 ℃ for 30 seconds, followed by 40 cycles of repeated procedure were conducted as follows: 95 ℃ for 3 s and 60 ℃ for 30 s. GAPDH was used as a control. Primers were synthesized by Sangon Biotechnology (Shanghai, China). Primers were as follows: HK2 forward: 5'-AAGGCTTCAAGGCATCTG-3', reverse: 5'-CCACAGGTCATCATAGTTCC-3'; GAPDH forward: 5'-ACAGTCAGCCGCATCTTCTT-3' reverse: 5'-GACAAGCTTCCCGTTCTCAG-3'. The relative mRNA was analyzed by using the formula $2^{-\Delta CT}$ [cycle threshold (CT) where $\Delta CT = CT (HK2) - CT (GAPDH)$] (8). All experiments were repeated three times.

Western blot

Cells were collected 48 h after infection. The total protein was dissociated in RIPA lysis buffer (Beyotime, Shanghai, China). The protein contents were measured using a BCA assay (Beyotime, Shanghai, China) and separated on 8% SDS-PAGE gel, and electrotransferred to PVDF membranes. PVDF membranes were blocked with 5% skim milk for 2 h in TBST and then incubated with initial antibodies at 4 ℃ overnight. The antibodies used were: mouse HK2 antibody (1:1,000; Abcam, Cambridge, USA) and mouse β-actin (1:10,000; Santa Cruz, California, USA). The secondary

antibody was peroxidase-conjugated Affinipure goat anti-mouse IgG (H + L) (ZSGB-BIO, Beijing, China). After incubation with a secondary antibody, the membranes were mixed with chemiluminescence reagents. Digital images were visualized though the electrochemilumine scene detection system (Invitrogen, USA).

X-ray IR

IR was performed with a 6 MV Siemens linear accelerator (23EX, Varian, USA) at a dose rate of 2 Gy/min.

CCK-8 proliferation assay

Three group cells (Control, Lv-shNC, Lv-shHK2) were washed with PBS after exposure to different doses of X-rays (0, 2, 4, 6, 8 Gy) and then suspended at a final concentration 5×10^3 per 100 µL and dispensed into 96-well plates. The plates were incubated at 37 ℃, 5% CO_2 for 46 h. Over the last 2 h, 10 µL CCK-8 was added to each well. The absorbance was measured at 495 nm using microplate reader (BioTek Instruments, Winooski, VT, USA) (9). These experiments were performed in triplicate.

Colony formation assay

Three group cells (Control, Lv-shNC, Lv-shHK2) were seeded into 6-well plates with a density of 500 cells/mL and cultured at 37 ℃ with 5% CO_2. Following the formation of sufficiently large clones, cells were stained with 0.1% crystal violet. The image was recorded and the number of colonies were counted.

Flow cytometry

The cells obtained from each of the three groups were seeded in 6-well plates at a density of 2× per well. Following 12 h of culturing, the cells were exposed to 4 Gy of X-ray and cultured for 48 h. The cells were then collected and suspended with a centrifuge containing trypsin without EDTA and washed in cold PBS. The concentration of cells was adjusted to 1×10^6 cells/mL, and then Annexin V-FICT and PI reagent were added.

Mouse xenograft BC models and treatment

Mice were divided into two groups: Lv-shNC group (n=8) and Lv-shHK2 group (n=8). Approximately 1× of lentivirus-infected MDA-MB-231 cells were collected in 150 µL of serum-free medium and were subcutaneously injected into the right axillary of 6-week-old female BALB/c mice. Mice were examined every 2 days and the formed tumors were measured using a micrometer. Mice in both groups (n=4) were irradiated once every 2 days over 5 times with a fractionated dose of 2 Gy using a medical linear accelerator (Varian 23EX; Varian Inc.) after the tumor volume was 5 mm (day 14) in diameter. The institutional and national guide for the care and use of laboratory animals was followed.

Micro PET/CT imaging of mice and quantitative analysis

^{18}F-FDG was provided by the Department of Nuclear Medicine of Ruijin hospital affiliated Shanghai Jiao Tong University and the radiochemical purities were more than 95%. ^{18}F-FDG PET/CT imaging was performed using a Micro-PET/CT scanner (Siemens; Siemens, Munich, Germany). The mice were not fed for at least for 6 h before ^{18}F-FDG PET/CT imaging and 5.5 MBq (150 uCi) of ^{18}F-FDG were injected into the tail vein 60 min before the scan start. Each mouse was then fixed in prone position at the midpoint of the visual filed on the scanning bed. One point five percent (1.5%) isoflurane with an O_2 flow rate of 2 L/min was prepared and mice anesthetized during the scanning period. The mice were first subjected to n CT scan and then to PET scan. The 3D images were reconstructed using a three dimensional ordered-subset expectation maximum algorithm (PSEM3D). For data analysis, the region of interest (ROI) was automatic sketched out using the image segmentation algorithm to segment the tumor region in the PET functional image using the CT image. The maximum standardized uptake value (SUVmax) of the ROI was calculated. The SUV was calculated as [decay-corrected activity (kBq) per milliliter of tissue volume)/ (injected ^{18}F-FDG activity (kBq)/body mass (g)].

Immunohistochemistry (IHC) examinations

Mice xenograft tumors were fixed with 10% neutral paraformaldehyde for 24 h. The tissues were embedded in paraffin, sectioned (5 µm), and stained with IHC. The antibody used was Ki67 (Santa Cruz Biotechnology, Santa Cruz, California, USA). The slides prepared from the tissue sections were examined under a light microscope by a photodocumentation facility (Olympus, Tokyo, Japan). The images were photographed in different magnification levels.
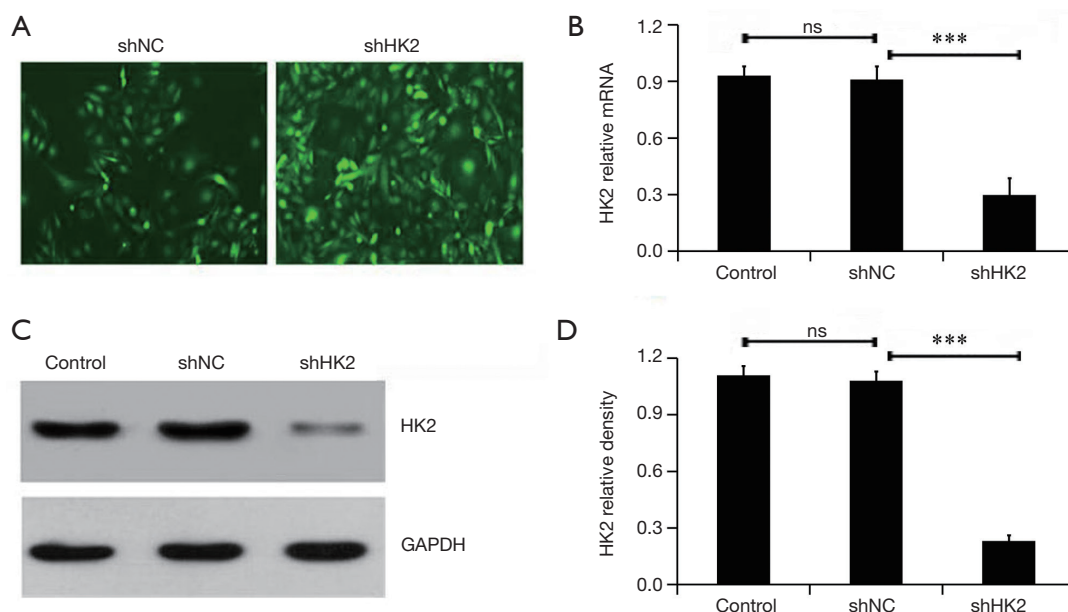
Figure 1 HK2 expression was assayed by qRT-PCR and western blot. (A) Fluorescent microscope (400×) was used to observe GFP positive cells. Approximately 90% cells were successfully infected with lentivirus in both groups; (B) HK2 mRNA was determined by qRT-PCR. HK2 mRNA was significantly reduced by treatment with Lv-shHK2 (***, P<0.01); (C) expression of HK2 protein was determined by western blot analysis. HK2 protein was significantly inhibited by Lv-shHK2. qRT-PCR, quantitative real-time polymerase chain reaction; GFP, green fluorescence; HK2, hexokinase 2.

For IHC staining, ×400 was used.

Statistical analysis

All data were expressed as mean ± SD. Statistical analysis was done using SPSS 17.0 and GraphPad Prism 5.0 Software. The difference between the two groups was analyzed by one-way ANOVA. The *t*-test was used to compare the two independent samples. P value <0.05 was considered statistically significant.

Results

Knockdown of HK2 expression suppresses cell proliferation and promotes cell apoptosis after IR in vitro

Lv-shNC or Lv-shHK2 containing GFP were infected into MDA-MB231 cells respectively, to explore the effect of HK2 on the radiosensitivity of BC MDA-MB231 cells. *Figure 1A* demonstrates that approximately 90.5%±8.7% cells were successfully infected with lentivirus though observing the GFP positive cells. The qRT-RCR and western blot methods were used to further detect the silencing effect of HK2 from mRNA and protein levels,

which were significantly reduced after administration with Lv-shHK2 (P<0.05, *Figure 1B,C*).

The effect of HK2 depletion on cell proliferation was detected by using CCK-8 assay. *Figure 2A* demonstrates the cells viability in the Lv-shHK2 group which displayed a decreased trend in a time and dose-dependent manner (P<0.05). In addition, the study further detected the cell apoptosis rate in different groups with or without exposure to IR and found that the apoptosis rate in the Lv-shHK2 group was higher than that in control group (*Figure 2B*). The colony formation ability with or without exposure to IR was significantly decreased in HK2 knockdown cells as compared with the NC group (*Figure 2C*).

^{18}F-FDG PET/CT in evaluating the radiation effect of TNBC xenografts by targeting HK2 gene

All the mice were randomly divided into two groups, Lv-shNC TNBC (n=8) and Lv-shHK2 TNBC (n=8) groups. TNBC xenograft models were observed within 2 weeks after tumor diameters were approximately 5 mm. Half of animals in the two groups with TNBC xenografts were treated with RT (daily fractions of 2 Gy for a total of 10 Gy).
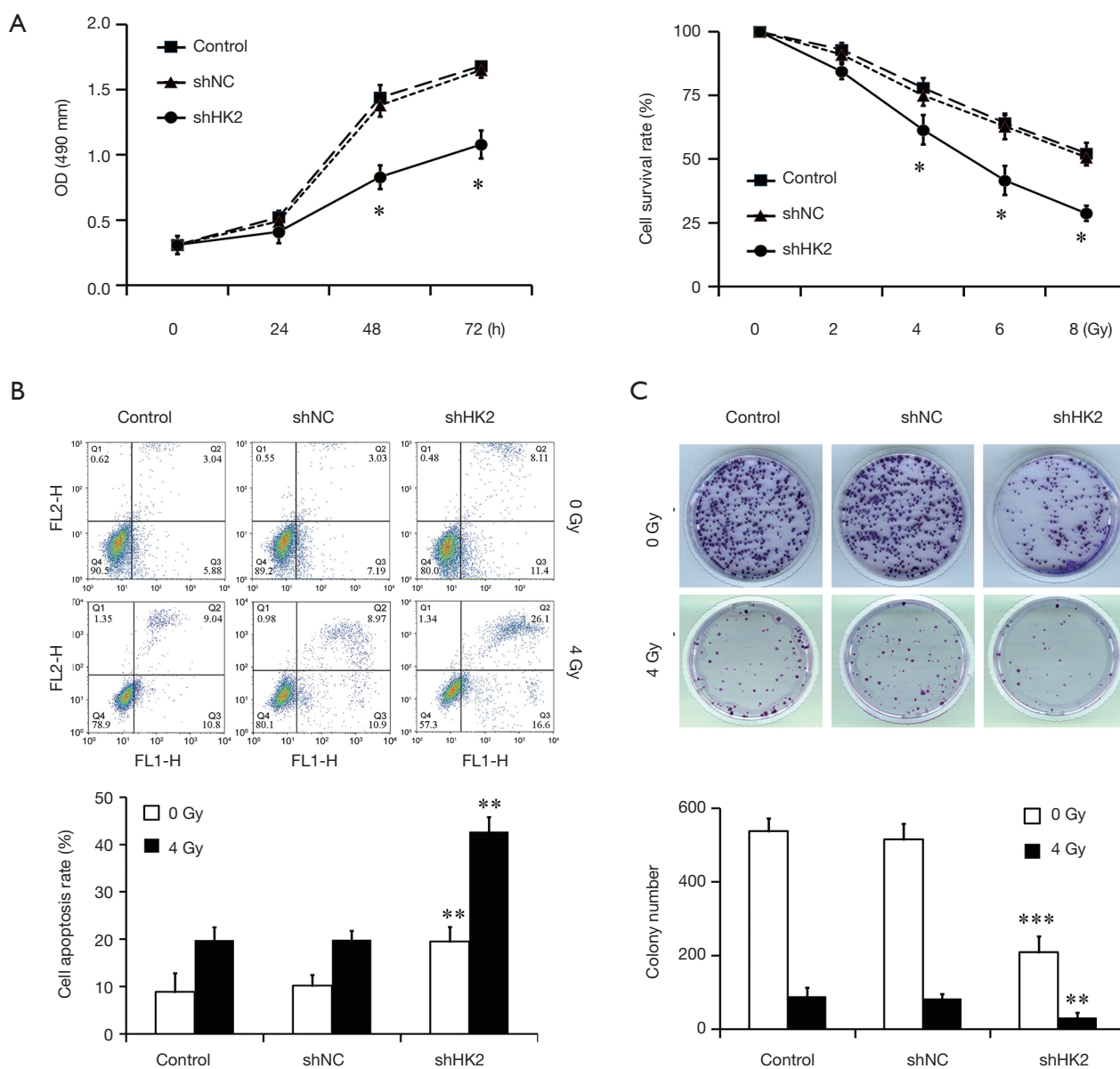
Figure 2 Downregulation of HK2 expression suppresses cell proliferation, colony formation and promotes cell apoptosis with or without IR. (A) CCK-8 proliferation assay was used to detect the cell proliferation. Compared with the Control and Lv-shNC groups, the cell survival rate in Lv-shHK2 group was significantly decreased (*, P<0.05); (B) the cell apoptosis rates in Lv-shHK2 group were significantly higher than those in the other two groups (**, P<0.01); (C) the colony formation ability with or without exposure to IR was significantly decreased in HK2 knockdown cells as compared with the other two groups (***, P<0.001 and **, P<0.01), using 0.1% crystal violet staining. IR, irradiation; HK2, hexokinase 2.

The study revealed that the growth rate of Lv-shHK2 was evidently slower than that of Lv-shNC after serial observation over 28 days. The tumors in Lv-shHK2 grew more slowly than those in Lv-shNC (P=0.0016, *Figure 3A*) after RT.

Before RT, on day 1 and 7 after RT, the mice bearing

Lv-shNC and Lv-shHK2 TNBC xenografts were subjected to ^{18}F-FDG microPET/CT scans respectively day 1 after treatment, the SUVmax in the Lv-shHK2 group showed a 20% decrease compared with that in the Lv-shNC group (*Figure 3B*). On day 7, SUVmax in Lv-shHK2 group was 42 % lower than that in the Lv-shNC group.
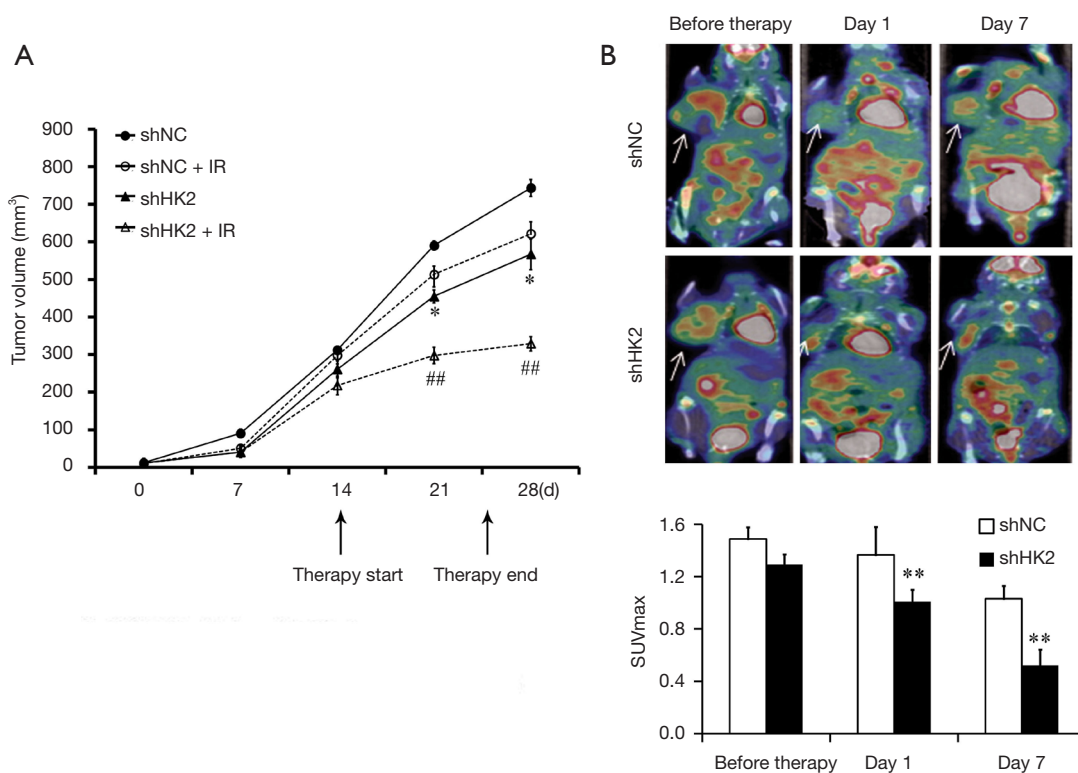
Figure 3 Evaluation of response to radiotherapy by targeting HK2 gene in TNBC xenografts. (A) The growth rates of Lv-shHK2 group with or without IR were significantly slower than Lv-shNC after a serial observation of 28 days (*, $P<0.05$ *vs.* shNC; ##, $P<0.01$ *vs.* shNC + IR); (B) ^{18}F-FDG micro PET/CT images of mice treated with radiotherapy at day 0, 1 and 7. Quantification of tumor uptake of ^{18}F-FDG is presented as SUVmax (**, $P<0.01$ *vs.* shNC). IR, irradiation; TNBC, triple-negative breast cancer; HK2, hexokinase 2; PET, positron emission tomography; CT, computed tomography.
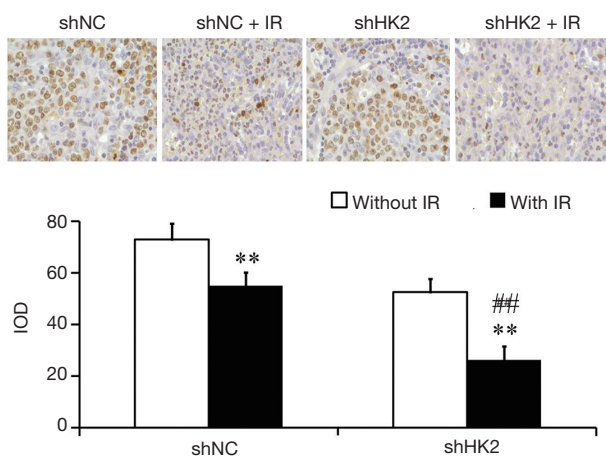
Figure 4 Ki67 immunohistochemical staining with or without IR (×400). (**, $P<0.01$ *vs.* without IR; ##, $P<0.01$ *vs.* shNC + IR). IR, irradiation.

Immunohistological examinations

Ki67 is closely related to proliferative and invasive ability of TNBC. The staining was most evident in the cell nuclei of the TNBC. Significant differences were noted between Lv-shNC and Lv-shHK2 groups. After RT, the proportions of positive cells were more obviously decreased in Lv-shHK2 group than in Lv-shNC (*Figure 4*).

Discussion

Approximately 70 years ago, Warburg demonstrated that malignant cells generally have accelerated glycolytic activity, even under aerobic conditions. He further suggested that it was a common characteristic observed in tumors. Subsequent reports have indicated that aerobic glycolysis is the result of a number of signature alterations (10). In line

with the Warburg effect, it has been shown that TNBC and HER2 positive BC possess higher levels of glycolytic activity than ER + BC cells (11,12). Thus, we hypothesized that if the initial steps of glycolysis would be suppressed in cancer cells, it would stop tumor anabolic processes. In this regard, HK2, the enzyme that catalyzes the first committed step of glycolysis seems to be an ideal target for cancer therapy. Studies have shown that HK2 is overexpressed in numerous types of cancer. This facilitates the proliferation and growth of cancer cells. However, the expression of HK2 is low or absent in most normal tissues (13). Various researchers have demonstrated that deletion of HK2 in mouse models inhibited tumor growth of BC and lung cancer, implying the feasibility of targeting HK2 for treatment of BC (14).

RT, combined with surgery and adjuvant chemotherapy is a key method in BC treatment. However, the radio-resistance is a major barrier that often leads to the failure of clinical therapy. Factors affecting the radiation resistance are varied an ill understood. Hypoxia is a general factor limiting the effectiveness of radiation therapy (15,16). Studies have shown that hypoxia has contributed to the recovery of impaired double stranded DNA induced by ionizing radiation. Second, lactic acid content in tumor cells often confers resistance. Tumor radiation dose was significantly positively correlated with the levels of lactic acid during RT. It is reported that inhibition of glycolysis can improve radiation sensitivity (17) and some products of glycolysis such as pyruvate, lactic acid, free radical scavengers can counteract free radical generated by RT, which causes reduced radiation sensitivity (18). Research has also shown that contents of lactic acid in cancer cells is associated with the low survival rates for patients and high metastasis rates of tumors (19).

The occurrence and development of malignant tumor cells is not only related to unlimited proliferation, but also related to the inhibition of apoptosis (20,21). In the study of human embryonic kidney cells and human cervical carcinoma cells, HK2 combined with mitochondria can block the interaction between pro apoptotic factor VDAC and Bax, thus inhibiting the apoptosis of cells (22). In addition, the reduced mitochondrial membrane permeability further prevents the release of cytochrome C (22). In this study, we investigated the relationship between *HK2* gene and radiosensitivity of BC. The results of cell proliferation, colony formation and cell apoptosis assays revealed that HK2 down-regulation could inhibit cell proliferation and colony formation and promote apoptosis with or without radiation therapy, indicating that inhibition

of the *HK2* gene improve radiation sensitivity. Moreover, the study evaluated the practicability of using ^{18}F-FDG PET/CT imaging to assess the efficacy of Lv-shHK2-based RT. The results also demonstrated that the tumor uptake of ^{18}F-FDG (SUVmax) after HK2 downregulation was significantly reduced compared with the control day 1 after treatment. However, there was no notable change in the tumor volume. On day 7 after treatment, the uptake of ^{18}F-FDG and tumor volume decreased more significantly in the Lv-shHK2 group. The study also compared the PET/CT results with the Ki67 immunohistochemical staining results, discovering that after RT, the proportions of positive cells were decreased in Lv-shHK2 group, indicating that downregulation of HK2 improves radiosensitivity of BC.

In summary, it is evident that downregulation of HK2 by lentiviral shRNA improves radiosensitivity of TNBC. ^{18}F-FDG PET/CT represents a potentially beneficial approach for evaluating the effect of mechanisms to increase radiosensitivity of cells.

Acknowledgments

Footnote

Conflicts of Interest: All authors have completed the ICMJE uniform disclosure form (available at http://dx.doi.org/10.21037/tcr.2019.01.37). The authors have no conflicts of interest to declare.

Ethical Statement: The authors are accountable for all aspects of the work in ensuring that questions related to the accuracy or integrity of any part of the work are appropriately investigated and resolved. The study followed the national or institutional guidelines for the care and use of animals. All animal experiments were approved by the Institutional Animal Care and Use Committees of the First Affiliated Hospital of Anhui Medical University (AMU-1-201633).

References

1. Torre LA, Bray F, Siegel RL, et al. Global cancer statistics, 2012. CA Cancer J Clin 2015;65:87-108.
2. Perou CM, Sorlie T, Eisen MB, et al. Molecular portraits of human breast tumours. Nature 2000;406:747-52.
3. Tischkowitz M, Brunet JS, Begin LR, et al. Use of immunohistochemical markers can refine prognosis in triple negative breast cancer. BMC Cancer 2007;7:134.
4. Nielsen TO, Hsu FD, Jensen K, et al. Immunohistochemical and clinical characterization of the basal-like subtype of invasive breast carcinoma. Clin Cancer Res 2004;10:5367-74.
5. Carey L, Winer E, Viale G, et al. Triple-negative breast cancer: disease entity or title of convenience? Nat Rev Clin Oncol 2010;7:683-92.
6. Warburg O. On the origin of cancer cells. Science 1956;123:309-14.
7. Mathupala SP, Rempel A, Pedersen PL. Glucose catabolism in cancer cells: identification and characterization of a marked activation response of the type II hexokinase gene to hypoxic conditions. J Biol Chem 2001;276:43407-12.
8. Li L, Liu M, Kang L, et al. HHEX: A Crosstalker between HCMV Infection and Proliferation of VSMCs. Front Cell Infect Microbiol 2016;6:169.
9. Wang L, Wu G, Qin X, et al. Expression of Nodal on Bronchial Epithelial Cells Influenced by Lung Microbes Through DNA Methylation Modulates the Differentiation of T-Helper Cells. Cell Physiol Biochem 2015;37:2012-22.
10. Semenza GL, Artemov D, Bedi A, et al. "The metabolism of tumors": 70 years later. Novartis Found Symp 2001;240:251-60.
11. Lanning NJ, Castle JP, Singh SJ, et al. Metabolic profiling of triple-negative breast cancer cells reveals metabolic vulnerabilities. Cancer Metab 2017;5:6.
12. Pelicano H, Zhang W, Liu J, et al. Mitochondrial dysfunction in some triple-negative breast cancer cell lines: role of mTOR pathway and therapeutic potential. Breast Cancer Res 2014;16:434.
13. Wolf A, Agnihotri S, Micallef J, et al. Hexokinase 2 is a key mediator of aerobic glycolysis and promotes tumor growth in human glioblastoma multiforme. J Exp Med 2011;208:313-26.
14. Patra KC, Wang Q, Bhaskar PT, et al. Hexokinase 2 is required for tumor initiation and maintenance and its systemic deletion is therapeutic in mouse models of cancer. Cancer Cell 2013;24:213-28.
15. Teicher BA. Hypoxia and drug resistance. Cancer Metastasis Rev 1994;13:139-68.
16. Brown JM. The hypoxic cell: a target for selective cancer therapy. Eighteenth Bruce F. Cain Memorial Award Lecture. Cancer Res 1999;59:5863-70.
17. Quennet V, Yaromina A, Zips D, et al. Tumor lactate content predicts for response to fractionated irradiation of human squamous cell carcinoma as in nude micen. Radiother Oncol 2006;81:130-5.
18. Meijer TW, Kaanders JH, Span PN, et al. Targeting hypoxia, HIF-1, and tumor glucose metabolism to improve radiotherapy efficacy. Clin cancer Res 2012;18:5585-94.
19. Walenta S, Mueller-Klieser WF. Lactate: mirror and motor of tumor malignancy. Semin Radiat Oncol 2004;14:267-74.
20. Hanahan D, Weinberg RA. The hallmarks of cancer. Cell 2000;100:57-70.
21. Mendoza FJ, Espino PS, Cann KL, et al. Anti-tumor chemotherapy utilizing peptide-based approaches - apoptotic pathways, kinases, and proteasome as targets. Arch Immunol Ther Exp (Warsz) 2005;53:47-60.
22. Bryson JM, Coy PE, Gottlob K, et al. Increased Hexokinase Activity, of Either Ectopic or Endogenous Origin, Protects Renal Epithelial Cells against Acute Oxidant-induced Cell Death. J Biol Chem 2002;277:11392-400.